Available online at www.sciencedirect.com
SCIENCE DIRECT®
Journal of Sound and Vibration 288 (2005) 293–306
JOURNAL OF SOUND AND VIBRATION
www.elsevier.com/locate/jsvi

Dynamic analysis of the linear discrete dynamic systems subjected to the initial conditions by using an FFT-based spectral analysis method

Usik Lee*, Sunghwan Kim, Jooyong Cho

Department of Mechanical Engineering, Inha University, 253 Yonghyun-Dong, Nam-Ku, Incheon 402-751, Republic of Korea

Received 2 June 2004; received in revised form 29 December 2004; accepted 10 January 2005
Available online 17 March 2005

Abstract

In this paper, a fast Fourier transforms (FFT)-based spectral analysis method is introduced for the dynamic analysis of the linear discrete dynamic systems subjected to the non-zero initial conditions. The FFT-based spectral analysis method is developed first for the one degree-of-freedom (dof) system and then extended to the multi-dof systems. To evaluate the accuracy and convergence of the FFT-based spectral analysis method, the forced vibration of a viscously damped 3-dof system is considered as an illustrative problem. The accuracy of the proposed FFT-based spectral analysis method is evaluated by comparing the forced vibration responses obtained by using the FFT-based spectral analysis method with the exact analytical solutions as well as with the numerical results obtained by using the Runge–Kutta method.

1. Introduction

The dynamic behavior of a system can be represented by a set of simultaneous second-order linear ordinary differential equations and the system is called the linear discrete dynamic system. For the distributed dynamic systems, an appropriate discretization process such as the finite element method can be used to represent them by the discrete dynamic system models.

*Corresponding author. Tel.: +82 32 860 7318; fax: +82 32 866 1434.
E-mail address: ulee@inha.ac.kr (U. Lee).

0022-460X/$ - see front matter © 2005 Elsevier Ltd. All rights reserved.
doi:10.1016/j.jsv.2005.01.014

For the linear discrete dynamic systems, a large number of analytical and numerical solution methods have been well developed. By virtue of impressive progress in computer technologies during last three decades, there have been developed diverse computer-based numerical methods to obtain satisfactory approximate solutions, especially for the coupled large degrees-of-freedom (dofs) systems. They may include various direct integration methods, the modal analysis methods, the discrete-time system methods, and the spectral analysis methods in which the fast Fourier transform (FFT) techniques are utilized. The first three are the time domain methods [1,2], while the FFT-based spectral element method (SAM) is a frequency-domain method [3–6].

In the FFT-based SAM, the dependent variables of a set of ordinary differential equations are all transformed into the frequency-domain by using the discrete Fourier transform (DFT) to transform the ordinary differential equations into a set of algebraic equations with frequency as a parameter. The algebraic equations are then solved for the Fourier (or spectral) components of dependent variables at each discrete frequency. As the final step, the time domain responses are reconstructed from the Fourier components by using the inverse discrete Fourier transform (IDFT). In practice, the FFT is used to carry out the DFT or IDFT. As the FFT is a remarkably efficient computer algorithm, it cannot only offer an enormous reduction in computer time but also increase the accuracy of solutions [4,7].

The FFT-based SAM has been known to be very useful especially in the following situations [4,6,7]. They are (1) when the excitation forces are so complicated that one has to use numerical integration to obtain the dynamic responses by using the excitation values at a discrete set of instants, (2) when the modern data acquisition systems are used, as in most experimental measurements, to store digitized data through the analogue-to-digital converters, (3) when it is significantly easier to measure the constitutive equation of a material in the frequency-domain rather than in the time domain, and (4) when the frequency-dependent spectral finite element (or dynamic stiffness matrix) model is used for a structure.

In Refs. [3–6,8], the FFT-based SAM has been well applied to the computation of the steady-state responses of dynamic systems. However, to the authors' best knowledge, the FFT-based SAM applications to the transient responses of dynamic systems have been mostly limited to the cases where all initial conditions are zero. By taking into account the initial conditions, Veletsos and Ventura [9,10] introduced a DFT-based procedure for calculating the transient response of a linear 1-dof system from its corresponding steady-state response to a periodic extension of the excitation. The procedure involves the superposition of a corrective, free vibration solution which effectively transforms the steady-state response to the desired transient response. Recently Mansur et al. [11,12] used the pseudo-force concept by taking into account the non-zero initial conditions in the DFT-based frequency-domain analysis of continuous media discretized by the FEM. Ref. [11] and the present paper solve the dynamic problem in modal coordinates, while Ref. [12] applies to the problems in both nodal and modal coordinates.

Thus, the purpose of this paper is to develop a new FFT-based SAM for the forced dynamic responses of the linear discrete dynamic systems subjected to non-zero initial conditions. The present FFT-based SAM is unique because it does not use the superposition of corrective, free vibration solution to match the initial conditions as in Refs. [9,10] or it does not used the pseudo-force concept to take into account the non-zero initial conditions as in Refs. [11,12]. To evaluate the convergence and accuracy of the FFT-based SAM, the forced vibration of a viscously damped 3-dofs vibration system is considered as an illustrative problem.

2. Discrete Fourier transform

A periodic function of time $x(t)$, with period T, can be always expressed as a Fourier series of the form

$$x(t) = a_0 + 2\sum_{n=0}^{\infty}\left(a_n \cos\frac{2\pi nt}{T} + b_n \sin\frac{2\pi nt}{T}\right) = \sum_{n=-\infty}^{\infty} X_n e^{i\omega_n t}, \tag{1}$$

where $\omega_n = n(2\pi/T) = n\omega_1$ are the discrete frequencies and X_n are constant Fourier components given by

$$X_n = a_n - ib_n = \frac{1}{T}\int_0^T x(t)e^{-i\omega_n t}\,dt \quad (n = 0, 1, 2, \ldots, \infty). \tag{2}$$

Eqs. (1) and (2) are the continuous Fourier transform pair for a periodic function.

Although $x(t)$ is a continuous function of time, it is often the case that only sampled values of the function are available, in the form of a discrete-time series $\{x(t_r)\}$. If N is the number of samples, all equally spaced with a time interval equal to $\Delta = T/N$, the discrete-time series are given by $x_r = x(t_r)$, where $t_r = r\Delta$ and $r = 0, 1, 2, \ldots, N-1$. The integral in Eq. (2) may be replaced approximately by the summation

$$X_n = \sum_{r=0}^{N-1} x(t_r)e^{-i\omega_n t_r} \quad (n = 0, 1, 2, \ldots, N-1) \tag{3}$$

which is the DFT of the discrete-time series $\{x_r\}$. Any typical value x_r of the series $\{x_r\}$ can be given by the inverse formula

$$x(t_r) = \frac{1}{N}\sum_{n=0}^{N-1} X_n e^{i\omega_n t_r} \quad (r = 0, 1, 2, \ldots, N-1) \tag{4}$$

which is the IDFT. Thus, Eqs. (3) and (4) represent the DFT–IFFT fair. Even though Eq. (3) is an approximation of Eq. (2), it is important to note that it allows all discrete time series $\{x_r\}$ to be regained *exactly* [6,7]. The Fourier components X_n in Eq. (4) are arranged as $X_{N-n} = X_n^*$, where $n = 0, 1, 2, \ldots, N/2$ and X_n^* represents the complex conjugate of X_n. Note that $X_{N/2}$ corresponds to the highest frequency $\omega_{N/2} = (N/2)\omega_1$, which is called the Nyquist frequency.

The FFT is an ingenious highly efficient computer algorithm developed to perform the numerical operations required for a DFT or IDFT, reducing the computing time drastically by the order $N/\log_2 N$. It should be pointed out that while the FFT-based spectral analysis uses a computer, it is not a numerical method in the usual sense, because the analytical descriptions of Eqs. (3) and (4) are still retained. Further details of DFT and FFT can be found in Newland [7].

3. Spectral analysis method for 1-dof dynamic systems

The DFT-based spectral analysis method will be developed first for the 1-dof dynamic system and then it will be extended to the multi-dofs dynamic systems in the next section.

As a representative example of the 1-dof dynamic systems, consider a viscously damped linear dynamic system represented by the equation of motion

$$\ddot{x} + 2\xi\Omega_0\dot{x} + \Omega_0^2 x = f(t) \tag{5}$$

and the initial conditions

$$x(0) = x_0, \quad \dot{x}(0) = \dot{x}_0. \tag{6}$$

In Eq. (5), ξ is the viscous damping ratio, Ω_0 is the natural frequency, and $f(t)$ is the excitation force. The total dynamic response of the system can be obtained by the sum of two parts: the steady-state response part and the transient part.

$$x(t) = x_p(t) + x_h(t). \tag{7}$$

The steady-state response part $x_p(t)$ corresponds to the particular solution of Eq. (5), which is mainly determined by excitation force $f(t)$. On the other hand, the transient response part $x_h(t)$, which is mainly determined by initial conditions, corresponds to the homogeneous solution of Eq. (5) and will vanish in general due to the damping as the time t increases indefinitely. The coefficients appeared in the transient response part $x_h(t)$ must be determined so as to satisfy all initial conditions.

3.1. Steady-state response

Based on the DFT theory, the external force $f(t)$ and the corresponding steady-state response $x_p(t)$ can be represented in the spectral forms (i.e., DFT forms) as

$$f(t_r) = \frac{1}{N}\sum_{n=0}^{N-1} F_n e^{i\omega_n t_r},$$

$$x_p(t_r) = \frac{1}{N}\sum_{n=0}^{N-1} P_n e^{i\omega_n t_r} \quad (r = 0, 1, 2, \ldots, N-1). \tag{8a, b}$$

Substituting Eq. (8) into Eq. (5) gives

$$P_n = Z_n F_n, \quad P_{N-n} = P_n^* \quad (n = 0, 1, 2, \ldots, N/2), \tag{9}$$

where Z_n is the complex frequency response function given by

$$Z_n = \frac{1}{(\Omega_0^2 - \omega_n^2) + i2\xi\Omega_0\omega_n}. \tag{10}$$

Once the Fourier components P_n are obtained from Eq. (9) for a given external force, the steady-state response in the time domain can be reconstructed by using the IFFT algorithm as

$$x_p(t) \Leftarrow \mathrm{IFFT}\{P_n\}. \tag{11}$$

The time derivative of the steady-state response $x_p(t)$ can be obtained from Eq. (8b) in the spectral form as

$$\dot{x}_p(t_r) = \frac{1}{N}\sum_{n=0}^{N-1} \bar{P}_n e^{i\omega_n t_r} \quad (r = 0, 1, 2, \ldots, N-1), \tag{12}$$

where

$$\bar{P}_n = (\mathrm{i}\omega_n)P_n, \quad \bar{P}_{N-n} = \bar{P}_n^* \quad (n = 0, 1, 2, \ldots, N/2). \tag{13}$$

3.2. Transient response

The transient response part $x_h(t)$ must satisfy the homogeneous equation of motion which can be reduced from Eq. (5) by enforcing $f(t) = 0$ as

$$\ddot{x}_h + 2\xi\Omega_0\dot{x}_h + \Omega_0^2 x_h = 0. \tag{14}$$

Substituting assumed solution $x_h(t) = \mathrm{e}^{\lambda t}$ into Eq. (14) yields a characteristic equation:

$$\Delta(\lambda) = \lambda^2 + 2\xi\Omega_0\lambda + \Omega_0^2 = (\lambda - \lambda_1)(\lambda - \lambda_2) = 0, \tag{15}$$

where λ_1 and λ_2 are the characteristic values and they are complex conjugates of each other (i.e., $\lambda_2 = \lambda_1^*$). The transient response part $x_h(t)$ can be then obtained in the form

$$x_h(t) = a\mathrm{e}^{\lambda_1 t} + a^*\mathrm{e}^{\lambda_1^* t}, \tag{16}$$

where a is the constant to be determined so as to satisfy the initial conditions Eq. (6), and a and a^* are complex conjugates of each other. The time derivative of $x_h(t)$ can be obtained from Eq. (16) as

$$\dot{x}_h(t) = a\lambda_1\mathrm{e}^{\lambda_1 t} + a^*\lambda_1^*\mathrm{e}^{\lambda_1^* t}. \tag{17}$$

Assume that $x_h(t)$ and $\dot{x}_h(t)$ can be expressed in the spectral forms as

$$\begin{aligned} x_h(t_r) &= \frac{1}{N}\sum_{n=0}^{N-1} H_n \mathrm{e}^{\mathrm{i}\omega_n t_r} \\ \dot{x}_h(t_r) &= \frac{1}{N}\sum_{n=0}^{N-1} \bar{H}_n \mathrm{e}^{\mathrm{i}\omega_n t_r} \quad (r = 0, 1, 2, \ldots, N-1). \end{aligned} \tag{18}$$

By applying Eq. (18) into Eq. (3), the Fourier components of $x_h(t)$ and $\dot{x}_h(t)$ can be obtained as

$$\begin{aligned} H_n &= \sum_{r=0}^{N-1} x_h(t_r)\mathrm{e}^{-\mathrm{i}\omega_n t_r} = aX_n + a^* Y_n, \\ \bar{H}_n &= \sum_{r=0}^{N-1} \dot{x}_h(t_r)\mathrm{e}^{-\mathrm{i}\omega_n t_r} = a\lambda_1 X_n + a^*\lambda_1^* Y_n, \end{aligned} \tag{19}$$

where

$$\begin{aligned} X_n &= \frac{1 - \mathrm{e}^{\alpha_n N}}{1 - \mathrm{e}^{\alpha_n}}, \quad \alpha_n = (\lambda_1 - \mathrm{i}\omega_n)\Delta, \\ Y_n &= \frac{1 - \mathrm{e}^{\beta_n N}}{1 - \mathrm{e}^{\beta_n}}, \quad \beta_n = (\lambda_1^* - \mathrm{i}\omega_n)\Delta. \end{aligned} \tag{20}$$

One should remind that $H_{N-n} = H_n^*$ and $\bar{H}_{N-n} = \bar{H}_n^*$, where $n = 0, 1, 2, \ldots, N/2$.

The constants a and a^* in Eq. (19) must be determined to satisfy the initial conditions Eq. (6). By using the general solution given by Eq. (7), the initial conditions Eq. (6) can be rewritten as

$$\begin{aligned} x_0 &= x_h(0) + x_p(0), \\ \dot{x}_0 &= \dot{x}_h(0) + \dot{x}_p(0). \end{aligned} \tag{21}$$

Substituting Eqs. (8), (12) and (18) into Eq. (21) yields

$$\begin{aligned} x_0 &= \frac{1}{N}\left(\sum_{n=0}^{N-1} H_n + \sum_{n=0}^{N-1} P_n\right), \\ \dot{x}_0 &= \frac{1}{N}\left(\sum_{n=0}^{N-1} \bar{H}_n + \sum_{n=0}^{N-1} \bar{P}_n\right). \end{aligned} \tag{22}$$

By substituting Eq. (19) into Eq. (22), one may obtain two algebraic equations for a and a^* as

$$\begin{aligned} \bar{X}a + \bar{Y}a^* &= d, \\ \lambda_1 \bar{X}a + \lambda_1^* \bar{Y}a^* &= v, \end{aligned} \tag{23}$$

where

$$\begin{aligned} \bar{X} &= \sum_{n=0}^{N-1} X_n, \quad \bar{Y} = \sum_{n=0}^{N-1} Y_n, \\ d &= Nx_0 - \sum_{n=0}^{N-1} P_n, \quad v = N\dot{x}_0 - \sum_{n=0}^{N-1} (\mathrm{i}\omega_n) P_n. \end{aligned} \tag{24}$$

The constant a can be solved from Eq. (23) in the form

$$a = \frac{\mathrm{i}}{2} R(\lambda_1^* d - v), \tag{25}$$

where

$$R = \frac{1}{\mathrm{Im}(\lambda_1)\bar{X}}. \tag{26}$$

In Eq. (26), Im $(\cdot)$ denotes the imaginary part of the complex number. Once the constant a (or a^*) is determined from Eq. (25), the transient response part in the time domain can be reconstructed by using the IFFT algorithm as

$$x_h(t) \Leftarrow \mathrm{IFFT}\{H_n\}. \tag{27}$$

Finally, as shown in Eq. (7), the total dynamic response of 1-dof dynamic system can be obtained by simply summing the steady-state response part $x_p(t)$ from Eq. (11) and the transient response part $x_h(t)$ from Eq. (27).

4. Spectral analysis method for multi-dofs dynamic systems

The forced vibration of a viscously damped m-dofs dynamic system can be represented by the matrix equation of motion

$$[\mathbf{M}]\{\ddot{\mathbf{u}}\} + [\mathbf{C}]\{\dot{\mathbf{u}}\} + [\mathbf{K}]\{\mathbf{u}\} = \{\mathbf{f}(t)\} \tag{28}$$

and the initial conditions

$$\{\mathbf{u}(0)\} = \{\mathbf{u}_0\} \quad \text{and} \quad \{\dot{\mathbf{u}}(0)\} = \{\dot{\mathbf{u}}_0\}, \tag{29}$$

where $\{\mathbf{u}(t)\}$ is the nodal dofs vector and $\{\mathbf{f}(t)\}$ is the nodal forces vector. The matrices [**M**], [**C**] and [**K**] are the mass matrix, damping matrix, and stiffness matrix, respectively. The total dynamic response of the system can be obtained by the sum of the steady-state response part $\{\mathbf{u}_p(t)\}$ and the transient response part $\{\mathbf{u}_h(t)\}$ as follows:

$$\{\mathbf{u}(t)\} = \{\mathbf{u}_p(t)\} + \{\mathbf{u}_h(t)\}. \tag{30}$$

4.1. Steady-state responses

Assume that the nodal forces vector $\{\mathbf{f}(t)\}$ and the steady-state responses vector $\{\mathbf{u}_p(t)\}$ can be represented in the spectral forms as

$$\{\mathbf{f}(t_r)\} = \frac{1}{N}\sum_{n=0}^{N-1}\{\mathbf{F}_n\}\mathrm{e}^{\mathrm{i}\omega_n t_r}$$

$$\{\mathbf{u}_p(t_r)\} = \frac{1}{N}\sum_{n=0}^{N-1}\{\mathbf{P}_n\}\mathrm{e}^{\mathrm{i}\omega_n t_r} \quad (r = 0, 1, 2, \ldots, N-1). \tag{31a, b}$$

Applying Eq. (31) into Eq. (28) yields

$$\{\mathbf{P}_n\} = [\mathbf{D}(\omega_n)]^{-1}\{\mathbf{F}_n\}, \quad \{\mathbf{P}_{N-n}\} = \{\mathbf{P}_n^*\} \quad (n = 0, 1, 2, \ldots, N/2), \tag{32}$$

where $[\mathbf{D}(\omega)]$ is the dynamic stiffness matrix defined by

$$[\mathbf{D}(\omega)] = \lfloor[\mathbf{K}] + \mathrm{i}\omega[\mathbf{C}] - \omega^2[\mathbf{M}]\rfloor. \tag{33}$$

From Eq. (31b), the time derivative of $\{\mathbf{u}_p(t)\}$ can be obtained as

$$\{\dot{\mathbf{u}}_p(t_r)\} = \frac{1}{N}\sum_{n=0}^{N-1}\{\bar{\mathbf{P}}_n\}\mathrm{e}^{\mathrm{i}\omega_n t_r}, \tag{34}$$

where

$$\{\bar{\mathbf{P}}_n\} = (\mathrm{i}\omega_n)\{\mathbf{P}_n\}, \quad \{\bar{\mathbf{P}}_{N-n}\} = \{\bar{\mathbf{P}}_n^*\} \quad (n = 0, 1, 2, \ldots, N/2). \tag{35}$$

Once the Fourier components $\{\mathbf{P}_n\}$ are computed from Eq. (32) for a given nodal forces vector $\{\mathbf{f}(t)\}$, the steady-state responses vector in the time domain can be reconstructed by using the IFFT algorithm as

$$\{\mathbf{u}_p(t)\} \Leftarrow \mathrm{IFFT}\{\mathbf{P}_n\}. \tag{36}$$

4.2. Transient responses

The transient responses vector $\{\mathbf{u}_h(t)\}$ must satisfy the homogeneous matrix equation of motion which can be reduced from Eq. (28) by enforcing $\{\mathbf{f}(t)\} = \mathbf{0}$ as follows:

$$[\mathbf{M}]\{\ddot{\mathbf{u}}_h\} + [\mathbf{C}]\{\dot{\mathbf{u}}_h\} + [\mathbf{K}]\{\mathbf{u}_h\} = \{\mathbf{0}\}. \tag{37}$$

The solution of Eq. (37) can be assumed in the form

$$\{\mathbf{u}_h(t)\} = [\mathbf{\Phi}]\{\mathbf{x}_h(t)\}, \tag{38}$$

where $[\mathbf{\Phi}]$ is the modal matrix which is the collection of normal modes satisfying the orthonormality properties

$$[\mathbf{\Phi}]^{\mathrm{T}}[\mathbf{M}][\mathbf{\Phi}] = [\mathbf{I}], \quad [\mathbf{\Phi}]^{\mathrm{T}}[\mathbf{K}][\mathbf{\Phi}] = [\mathbf{\Omega}^2], \tag{39a,b}$$

where $[\mathbf{I}]$ is the identity matrix and $[\mathbf{\Omega}^2]$ is the diagonal matrix defined by

$$[\mathbf{\Omega}^2] = \mathrm{diag}[\Omega_1^2 \ \Omega_2^2 \ \cdots \ \Omega_m^2], \tag{40}$$

where $\Omega_1 \leqslant \Omega_2 \leqslant \cdots \leqslant \Omega_m$ are the natural frequencies.

By substituting Eq. (38) into Eq. (37) and by applying Eq. (39), one may obtain a set of decoupled modal equations as

$$\ddot{x}_{hk} + 2\xi_k \Omega_k \dot{x}_{hk} + \Omega_k^2 x_{hk} = 0 \quad (k = 1, 2, \ldots, m), \tag{41}$$

where ξ_k is the kth modal damping ratio. Each modal equation of Eq. (41) is essentially the same as Eq. (14). Thus, the solution procedure introduced in the preceding section for 1-dof dynamic systems can be equally applied to Eq. (41).

First assume that the characteristic equation for the kth modal equation can be expressed as

$$\Delta_k(\lambda) = \lambda^2 + 2\xi_k \Omega_k \lambda + \Omega_k^2 = (\lambda - \lambda_{k1})(\lambda - \lambda_{k2}) = 0, \tag{42}$$

where λ_{k1} and λ_{k2} are the complex conjugates of each other, that is $\lambda_{k2} = \lambda_{k1}^*$. The transient part of modal response $x_{hk}(t)$ and its derivative with respect to time can be then readily obtained in the forms

$$x_{hk}(t) = a_k e^{\lambda_{k1} t} + a_k^* e^{\lambda_{k1}^* t}$$

$$\dot{x}_{hk}(t) = a_k \lambda_{k1} e^{\lambda_{k1} t} + a_k^* \lambda_{k1}^* e^{\lambda_{k1}^* t} \quad (k = 1, 2, \ldots, m), \tag{43}$$

where the constants a_k and a_k^* must be determined to satisfy the initial conditions given by Eq. (29).

Represent $x_{hk}(t)$ and $\dot{x}_{hk}(t)$ into the spectral forms as

$$x_{hk}(t_r) = \frac{1}{N} \sum_{n=0}^{N-1} H_{kn} e^{\mathrm{i}\omega_n t_r}$$

$$\dot{x}_{hk}(t_r) = \frac{1}{N} \sum_{n=0}^{N-1} \bar{H}_{kn} e^{\mathrm{i}\omega_n t_r} \quad (r = 0, 1, 2, \ldots, N-1). \tag{44}$$

By using Eq. (3), the Fourier components H_{kn} and $\bar{H}_{kn}$ in Eq. (44) can be expressed as

$$H_{kn} = \sum_{r=0}^{N-1} x_{hk}(t_r)\mathrm{e}^{-\mathrm{i}\omega_n t_r} = a_k X_{kn} + a_k^* Y_{kn},$$
$$\bar{H}_{kn} = \sum_{r=0}^{N-1} \dot{x}_{hk}(t_r)\mathrm{e}^{-\mathrm{i}\omega_n t_r} = a_k \lambda_{k1} X_{kn} + a_k^* \lambda_{k1}^* Y_{kn}, \tag{45}$$

where

$$X_{kn} = \frac{1-\mathrm{e}^{\alpha_{kn}N}}{1-\mathrm{e}^{\alpha_{kn}}}, \quad \alpha_{kn} = (\lambda_{k1} - \mathrm{i}\omega_n \Delta),$$
$$Y_{kn} = \frac{1-\mathrm{e}^{\beta_{kn}N}}{1-\mathrm{e}^{\beta_{kn}}}, \quad \beta_{kn} = (\lambda_{k1}^* - \mathrm{i}\omega_n)\Delta. \tag{46}$$

The Fourier components satisfy the relations $H_{k(N-n)} = H_{kn}^*$ and $\bar{H}_{k(N-n)} = \bar{H}_{kn}^*$, where $n = 0, 1, 2, \ldots, N/2$.

Collect $x_{hk}(t)$ and $\dot{x}_{hk}(t)$ given by Eq. (44) to form the vectors as

$$\{\mathbf{x}_h(t_r)\} = \frac{1}{N}\sum_{n=0}^{N-1} \{\mathbf{H}_n\}\mathrm{e}^{\mathrm{i}\omega_n t_r}$$
$$\{\dot{\mathbf{x}}_h(t_r)\} = \frac{1}{N}\sum_{n=0}^{N-1} \{\bar{\mathbf{H}}_n\}\mathrm{e}^{\mathrm{i}\omega_n t_r} \quad (r = 0, 1, 2, \ldots, N-1), \tag{47a, b}$$

where

$$\{\mathbf{x}_h\} = \{x_{h1}\ x_{h2} \quad \cdots \quad x_{hm}\}^{\mathrm{T}},$$
$$\{\dot{\mathbf{x}}_h\} = \{\dot{x}_{h1}\ \dot{x}_{h2} \quad \cdots \quad \dot{x}_{hm}\}^{\mathrm{T}} \tag{48}$$

and

$$\{\mathbf{H}_n\} = \{H_{1n}\ H_{2n} \quad \cdots \quad H_{mn}\}^{\mathrm{T}}$$
$$\{\bar{\mathbf{H}}_n\} = \{\bar{H}_{1n}\ \bar{H}_{2n} \quad \cdots \quad \bar{H}_{mn}\}^{\mathrm{T}}. \tag{49}$$

Applying Eq. (47a) into Eq. (38) gives

$$\{\mathbf{u}_h(t_r)\} = \frac{1}{N}[\mathbf{\Phi}]\sum_{n=0}^{N-1} \{\mathbf{H}_n\}\mathrm{e}^{\mathrm{i}\omega_n t_r} \quad (r = 0, 1, 2, \ldots, N-1). \tag{50}$$

Differentiate Eq. (38) with respect to time and then apply Eq. (47b) to obtain

$$\{\dot{\mathbf{u}}_h(t_r)\} = \frac{1}{N}[\mathbf{\Phi}]\sum_{n=0}^{N-1} \{\bar{\mathbf{H}}_n\}\mathrm{e}^{\mathrm{i}\omega_n t_r} \quad (r = 0, 1, 2, \ldots, N-1). \tag{51}$$

Substituting the general solution Eq. (30) into the initial conditions Eq. (29) yields the relations as

$$\{\mathbf{u}_0\} = \{\mathbf{u}_p(0)\} + \{\mathbf{u}_h(0)\},$$

$$\{\dot{\mathbf{u}}_0\} = \{\dot{\mathbf{u}}_p(0)\} + \{\dot{\mathbf{u}}_h(0)\}. \tag{52}$$

Applying Eqs. (31b), (34), (50) and (51) into Eq. (52) gives

$$\{\mathbf{u}_0\} = \frac{1}{N}\left(\sum_{n=0}^{N-1}\{\mathbf{P}_n\} + [\mathbf{\Phi}]\sum_{n=0}^{N-1}\{\mathbf{H}_n\}\right),$$
$$\{\dot{\mathbf{u}}_0\} = \frac{1}{N}\left(\sum_{n=0}^{N-1}\{\bar{\mathbf{P}}_n\} + [\mathbf{\Phi}]\sum_{n=0}^{N-1}\{\bar{\mathbf{H}}_n\}\right). \tag{53}$$

By using Eq. (45), Eq. (49) can be rewritten as

$$\{\mathbf{H}_n\} = [\mathbf{X}_n]\{\mathbf{a}\} + [\mathbf{Y}_n]\{\mathbf{a}^*\},$$
$$\{\bar{\mathbf{H}}_n\} = [\mathbf{\Lambda}_1][\mathbf{X}_n]\{\mathbf{a}\} + [\mathbf{\Lambda}_1^*][\mathbf{Y}_n]\{\mathbf{a}^*\}, \tag{54a, b}$$

where

$$\{\mathbf{a}\} = \{a_1 \;\; a_2 \;\; \cdots \;\; a_m\}^{\mathrm{T}},$$
$$\{\mathbf{a}^*\} = \{a_1^* \;\; a_2^* \;\; \cdots \;\; a_m^*\}^{\mathrm{T}},$$
$$[\mathbf{X}_n] = \mathrm{diag}[X_{1n} \;\; X_{2n} \;\; \cdots \;\; X_{mn}],$$
$$[\mathbf{Y}_n] = \mathrm{diag}[Y_{1n} \;\; Y_{2n} \;\; \cdots \;\; Y_{mn}],$$
$$[\mathbf{\Lambda}_1] = \mathrm{diag}[\lambda_{11} \;\; \lambda_{21} \;\; \cdots \;\; \lambda_{m1}],$$
$$[\mathbf{\Lambda}_1^*] = \mathrm{diag}[\lambda_{11}^* \;\; \lambda_{21}^* \;\; \cdots \;\; \lambda_{m1}^*]. \tag{55}$$

Substituting Eq. (54a,b) into Eq. (53) gives

$$[\bar{\mathbf{X}}]\{\mathbf{a}\} + [\bar{\mathbf{Y}}]\{\mathbf{a}^*\} = \{\mathbf{d}\},$$
$$[\mathbf{\Lambda}_1][\bar{\mathbf{X}}]\{\mathbf{a}\} + [\mathbf{\Lambda}_1^*][\bar{\mathbf{Y}}]\{\mathbf{a}^*\} = \{\mathbf{v}\}, \tag{56}$$

where

$$[\bar{\mathbf{X}}] = \sum_{n=0}^{N-1}[\mathbf{X}_n],$$
$$[\bar{\mathbf{Y}}] = \sum_{n=0}^{N-1}[\mathbf{Y}_n],$$
$$\{\mathbf{d}\} = [\mathbf{\Phi}]^{\mathrm{T}}[\mathbf{M}]\left(N\{\mathbf{u}_0\} - \sum_{n=0}^{N-1}\{\mathbf{P}_n\}\right),$$
$$\{\mathbf{v}\} = [\mathbf{\Phi}]^{\mathrm{T}}[\mathbf{M}]\left(N\{\dot{\mathbf{u}}_0\} - \sum_{n=0}^{N-1}(\mathrm{i}\omega_n)\{\mathbf{P}_n\}\right). \tag{57a–d}$$

In Eq. (57c) and (57d), $[\mathbf{\Phi}]^{-1}$ is replaced with $[\mathbf{\Phi}]^{\mathrm{T}}[\mathbf{M}]$ by the use of Eq. (39a).

The constants vector $\{\mathbf{a}\}$ or $\{\mathbf{a}^*\}$ can be solved from Eq. (56) in the form

$$\{\mathbf{a}\} = \frac{\mathrm{i}}{2}[\mathbf{R}]([\mathbf{\Lambda}_1^*]\{\mathbf{d}\} - \{\mathbf{v}\}), \tag{58}$$

where

$$[\mathbf{R}] = \mathrm{diag}[R_1 \ R_2 \ \cdots \ R_m] \tag{59}$$

with

$$R_k = \frac{1}{\mathrm{Im}(\lambda_{k1})\bar{X}_k}, \quad \bar{X}_k = \sum_{n=0}^{N-1} X_{kn} \quad (k = 1, 2, \ldots, m). \tag{60}$$

Once $\{\mathbf{a}\}$ is computed from Eq. (58) by using given initial conditions, the Fourier components $\{\mathbf{H}_n\}$ are computed first from Eq. (54a) and then the IFFT algorithm is used to compute $\{\mathbf{x}_h(t)\}$ as

$$\{\mathbf{x}_h(t)\} \Leftarrow \mathrm{IFFT}\{\mathbf{H}_n\}. \tag{61}$$

The transient responses vector in the time domain is then obtained by substituting the result from Eq. (61) into Eq. (38) as follows:

$$\{\mathbf{u}_h(t)\} = [\mathbf{\Phi}]\{\mathbf{x}_h(t)\} = [\mathbf{\Phi}]\mathrm{IFFT}\{\mathbf{H}_n\}. \tag{62}$$

As the final step, the total dynamic responses of the system are obtained by summing the steady-state responses vector $\{\mathbf{u}_p(t)\}$ from Eq. (36) and the transient responses vector $\{\mathbf{u}_h(t)\}$ from Eq. (62).

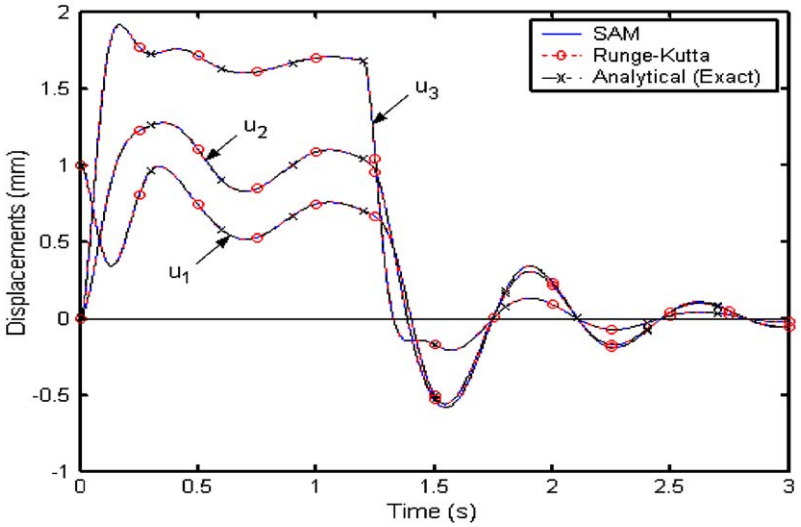

Fig. 1. Comparison of the time histories $u_1(t), u_2(t)$ and $u_3(t)$ obtained by different solution methods.

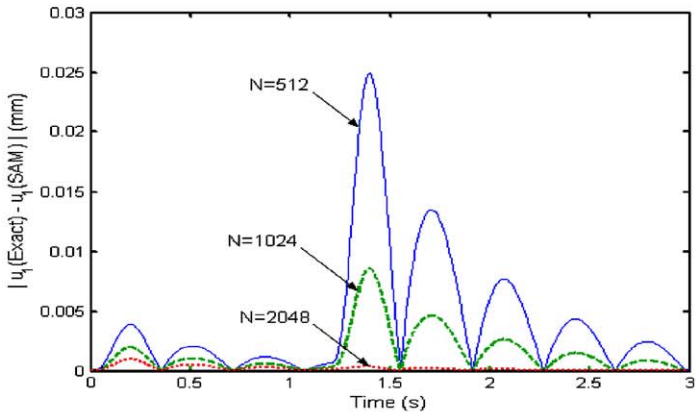

(a) Time history of the error in $u_1(t)$

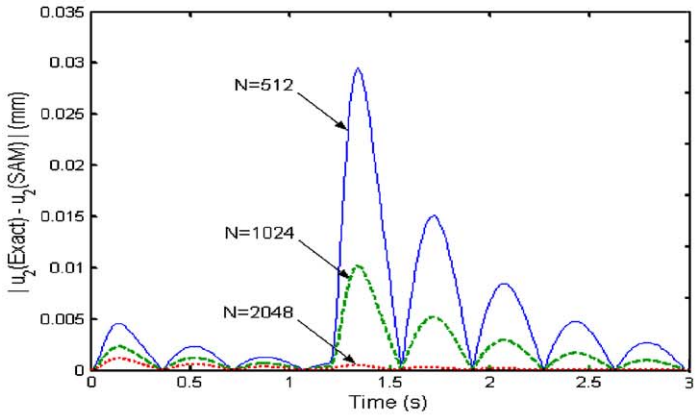

(b) Time history of the error in $u_2(t)$

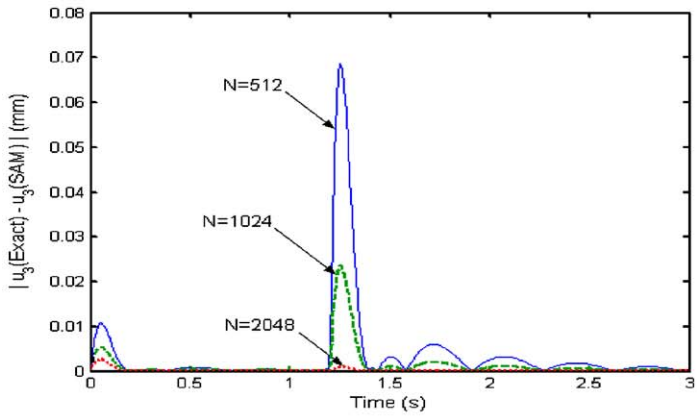

(c) Time history of the error in $u_3(t)$

Fig. 2. Convergence of the time histories as the number of samples N is increased.

Table 1
Comparison of the CPU times and the time-averaged errors

Analysis methods		SAM (Present)			Runge–Kutta method	
		$N = 512$	$N = 1024$	$N = 2048$	$\Delta t = 0.0005$(s)	$\Delta t = 0.0001$(s)
CPU time (s)		0.182	0.323	0.792	0.984	3.428
Time-averaged % error	$u_1(t)$	8.061	2.880	0.150	5.669	0.123
	$u_2(t)$	7.800	2.453	0.140	5.840	0.124
	$u_3(t)$	6.975	2.344	0.157	5.845	0.589

5. Numerical example

To evaluate the present FFT-based SAM, a viscously damped three dofs vibration system is considered as an illustrative problem, which is represented by

$$\begin{bmatrix} m & 0 & 0 \\ 0 & m & 0 \\ 0 & 0 & m/2 \end{bmatrix} \begin{Bmatrix} \ddot{u}_1 \\ \ddot{u}_2 \\ \ddot{u}_3 \end{Bmatrix} + \begin{bmatrix} 3c & -2c & 0 \\ -2c & 3c & -c \\ 0 & -c & 3c \end{bmatrix} \begin{Bmatrix} \dot{u}_1 \\ \dot{u}_2 \\ \dot{u}_3 \end{Bmatrix} + \begin{bmatrix} 3k & -2k & 0 \\ -2k & 3k & -k \\ 0 & -k & 3k \end{bmatrix} \begin{Bmatrix} u_1 \\ u_2 \\ u_3 \end{Bmatrix} = \begin{Bmatrix} 0 \\ 0 \\ f(t) \end{Bmatrix}, \tag{63}$$

where $m = 10\,\mathrm{kg}, c = 40\,\mathrm{N\,s/m}, k = 1000\,\mathrm{N/m}$, and $f(t) = 4[1 - s(t - 1.2)]N$, where $s(t)$ represents the unit step function. The initial conditions are given by

$$\begin{aligned} \{u_1, u_2, u_3\} &= \{1, 0, 0\}\,(\mathrm{mm}), \\ \{\dot{u}_1, \dot{u}_2, \dot{u}_3\} &= \{0, 1, 0\}\,(\mathrm{mm/s}). \end{aligned} \tag{64}$$

In Fig. 1, the time histories of u_1, u_2 and u_3 obtained by the present FFT-based SAM are compared with exact analytical results obtained by the modal analysis method as well as with the numerical results obtained by the Runge–Kutta method. To obtain sufficiently accurate time histories within 0.05% time-averaged errors, the DFT period $T = 5\,\mathrm{s}$ and the number of samples $N = 2048$ are used for the SAM, while the time step size of 0.0001 s is used for Runge–Kutta method. The present FFT-based SAM results are found to be almost identical to the exact analytical results.

Fig. 2 demonstrates the convergence of the present FFT-based SAM results as the number of samples N is increased. As also shown in Fig. 1, Fig. 2 certainly shows that the time histories obtained by the present FFT-based SAM converge enough to the exact analytical results when the number of samples N is increased up to 2048.

Table 1 shows the comparison of the CPU times and the time-averaged errors of time histories, with varying the number of samples N and the time increment step for the present FFT-based SAM and the Runge–Kutta method, respectively. The present FFT-based SAM is found to require less CPU times than the Runge–Kutta method to obtain the time histories of the same order of averaged errors.

6. Conclusions

This paper introduces a new FFT-based SAM for calculating the forced dynamic responses of the linear discrete dynamic systems with non-zero initial conditions. The proposed method seems to be very useful especially when the excitation forces are provided as the measured digitized data and when the structural properties such as the stiffness and damping coefficients are provided as the frequency-dependent data. The accuracy and convergence of the proposed FFT-based SAM are evaluated by comparing the forced vibration responses of a viscously damped three dofs vibration system obtained by using the FFT-based SAM with the exact analytical solutions as well as with the numerical results obtained by using the Runge–Kutta method. It is also shown that the proposed FFT-based SAM provides very accurate results with requiring less CPU time for the example problem when compared with the Runge–Kutta method.

Acknowledgements

This work was supported by 2005 Inha University Research Grant.

References

[1] L. Meirovitch, *Computational Methods in Structural Dynamics*, Sijthoff & Noodhoff, Netherlands, 1980.
[2] D.E. Newland, *Mechanical Vibration Analysis and Computation*, Wiley, New York, 1989.
[3] G.V. Narayanan, D.E. Beskos, Use of dynamic influence coefficients in forced vibration problems with the aid of fast Fourier transform, *Computers & Structures* 9 (1978) 145–150.
[4] J.F. Doyle, *Wave Propagation in Structures, Spectral Analysis Using Fast Discrete Fourier Transforms*, Springer, New York, 1997.
[5] U. Lee, J. Kim, A.Y.T. Leung, The spectral element method in structural dynamics, *The Shock and Vibration Digest* 32 (2000) 451–465.
[6] J.H. Ginsberg, *Mechanical and Structural Vibrations, Theory and Applications*, Wiley, New York, 2001.
[7] D.E. Newland, *Random Vibrations, Spectral and Wavelet Analysis*, Longman, New York, 1993.
[8] J.L. Humar, H. Xia, Dynamic response analysis in the frequency domain, *Earthquake Engineering and Structural Dynamics* 22 (1993) 1–12.
[9] A.S. Veletsos, C.E. Ventura, Efficient analysis of dynamic response of linear systems, *Earthquake Engineering and Structural Dynamics* 12 (1984) 521–536.
[10] A.S. Veletsos, C.E. Ventura, Dynamic analysis of structures by the DFT method, *Journal of Structural Engineering* 111 (1985) 2625–2642.
[11] W.J. Mansur, J.A.M. Carrer, W.G. Ferreira, A.M. Claret de Gouveia, F. Venancio-Filho, Time-segmented frequency-domain analysis for non-linear multi-degree-of-freedom structural systems, *Journal of Sound and Vibration* 237 (2000) 457–475.
[12] W.J. Mansur, D. Soares Jr., M.A.C. Ferro, Initial conditions in frequency-domain analysis: the FEM applied to the scalar wave equation, *Journal of Sound and Vibration* 270 (2004) 767–780.